

# Acceleration of Genetic Algorithm for Peak Power Reduction of OFDM Signal

Noritaka Shigei, Hiromi Miyajima, Keisuke Ozono, and Kentaro Araki

**Abstract**—Orthogonal frequency division multiplexing (OFDM) is superior in spectral efficiency and is widely used in today's digital communication. One of the drawbacks of OFDM is that the peak-to-average power ratio (PAPR) of the transmitted signal tends to be high. In order to overcome this problem, peak power reduction methods based on tone injection have been proposed. The peak power reduction problem solved with tone injection is a combinatorial problem. In this paper, we apply genetic algorithm (GA) to the reduction method based on tone injection. In order to reduce to the computation time, the proposed GA method utilizes a fitness table. For the fitness table, two types of implementation are presented. The effectiveness of the GA method is demonstrated by numerical simulations in terms of PAPR, bit error rate (BER) and power spectral density (PSD). Further, the numerical simulation shows that the proposed GA method is superior in terms of computation time compared to conventional GA and random search. Especially, it is shown that the hash-based fitness table is most effective for the acceleration of GA.

**Index Terms**—OFDM, PAPR, tone injection, genetic algorithm, tree-structured table, hash table.

## I. INTRODUCTION

RECENT advance in digital signal processing technology demands faster wireless communication. Orthogonal frequency division multiplexing (OFDM) [1] is superior in spectral efficiency and is widely used in today's digital communication. One of the drawbacks of OFDM is that the peak-to-average power ratio (PAPR) of the transmitted signal tends to be high. In order to overcome this problem, various peak power reduction methods have been proposed [2], [3], [4], [5], [6], [7]. Tone injection is an effective technique to overcome the PAPR problem [6], [7]. The peak power reduction problem solved with tone injection is a combinatorial problem. In [6], a greedy searching algorithm has been proposed. Its main drawback is to easily get a stack shallow local minimum. In [7], the solution space is reasonably reduced by introducing some constraints into the tone injection technique, and a peak power reduction method based on neural network (NN). However, the reduction performance is high.

In this paper, we apply genetic algorithm (GA) to the reduction method based on tone injection. In order to reduce

Manuscript received January 24, 2011. This work was supported by Grant-in-Aid for Scientific Research (C) (No.20500070) of Ministry of Education, Culture, Sports, Science and Technology of Japan.

N. Shigei is with Graduate School of Science and Engineering, Kagoshima University, 1-21-40 Korimoto, Kagoshima 890-0065, Japan (corresponding author to provide phone/fax: +81-99-285-8416; email: shigei@eee.kagoshima-u.ac.jp).

H. Miyajima is with Graduate School of Science and Engineering, Kagoshima University, 1-21-40 Korimoto, Kagoshima 890-0065, Japan (email: miya@eee.kagoshima-u.ac.jp).

K. Ozono was with Graduate School of Science and Engineering, Kagoshima University, 1-21-40 Korimoto, Kagoshima 890-0065, Japan (email: k6140848@kadai.jp).

K. Araki is with Faculty of Engineering, Kagoshima University, 1-21-40 Korimoto, Kagoshima 890-0065, Japan (email: k2287401@kadai.jp)

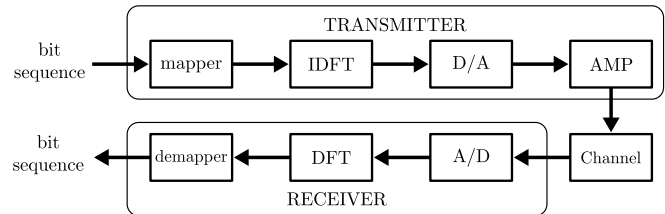


Fig. 1. Flow of OFDM from a Transmitting End to a Receiving End

to the computation time, the proposed GA method utilizes a fitness table. In [13], we have proposed a tree-structured fitness table. As a new contribution of this paper, we implement the fitness table by using a hash table. The effectiveness of the GA method is demonstrated by numerical simulations in terms of PAPR, bit error rate (BER) and power spectral density (PSD). We also investigate effective fitness functions and crossover operators. It is shown that a uniform crossover operation is most effective. Further, it is shown that our GA method is superior in terms of computation time compared to conventional GA and random search. Especially, it is shown that the hash-based fitness table is most effective for the acceleration of GA.

## II. OFDM AND TONE INJECTION

### A. OFDM

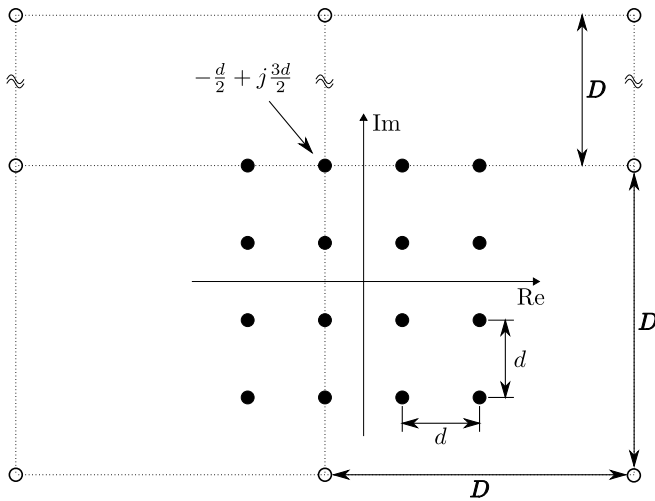
OFDM uses multiple subcarriers that are orthogonal to each other. Let  $T$  be the OFDM symbol time. The subcarriers are spaced  $1/T$  Hz apart from each other. The flow of OFDM from a transmitting end to a receiving end is shown in Fig.1.

At the transmitter side, a bit sequence  $b_{L-1}, b_{L-2}, \dots, b_0$  to be transmitted is converted into a sequence of complex symbols  $X_0, X_1, \dots, X_{N-1}$  by mapper. In this conversion, each  $M$ -bit subsequence in  $L$ -bit sequence is mapped to a complex number according to the used digital modulation scheme such as phase-shift keying (PSK) and quadrature amplitude modulation (QAM). When using  $M$ -QAM,  $X_n$  represents  $\log_2 M$ -bit subsequence  $b_{L-m \cdot n-1}, b_{L-m \cdot n-2}, \dots, b_{L-m \cdot n-M}$ , where  $L = M \log_2 M$  and  $m = \log_2 M$ . Samples of OFDM signal  $Y_0, Y_1, \dots, Y_{N-1}$  are generated by IDFT (Inverse Discrete Fourier Transform) as follows:

$$Y_n = \frac{1}{N} \sum_{k=0}^{N-1} X_k e^{j \frac{2\pi}{N} nk}. \quad (1)$$

The IDFT operation can be performed by IFFT (Inverse Fast Fourier Transformation) in  $O(N \log N)$  steps. The samples are converted to an analog signal, and then the signal is amplified and is fed to the transmission channel.

The demodulation process is performed in reverse order of transmitter's operations. From the received OFDM signal,  $N$


 Fig. 2. Symbol Relocation of Tone Injection for 16-QAM and  $\rho = 1$ 

samples  $\tilde{Y}_0, \tilde{Y}_1, \dots, \tilde{Y}_{N-1}$  are extracted with  $T/N$  sampling interval. Symbols  $\tilde{X}_0, \tilde{X}_1, \dots, \tilde{X}_{N-1}$  are restored by DFT (Discrete Fourier Transform) as follows:

$$\tilde{X}_n = \sum_{k=0}^{N-1} \tilde{Y}_k e^{-j\frac{2\pi}{N}nk}. \quad (2)$$

The restored symbol sequence  $\tilde{X}_0, \tilde{X}_1, \dots, \tilde{X}_{N-1}$  is converted to a bit sequence  $\tilde{b}_{L-1}, \tilde{b}_{L-2}, \dots, \tilde{b}_0$ . If  $\tilde{X}_n = X_n$  for all  $n \in \{0, 1, \dots, N-1\}$ , the receiver retrieves the transmitted bit sequence  $b_{L-1}, b_{L-2}, \dots, b_0$  with no error, that is, for all  $l \in \{0, 1, \dots, L-1\}$ ,  $\tilde{b}_l = b_l$ .

The OFDM signal often has a very high peak power compared to its average power, because the signal is produced as a synthetic signal of a number of subcarriers. The degree of the peak power is evaluated by peak-to-average power ratio (PAPR) defined as follows:

$$\text{PAPR} = \frac{\max_{0 \leq k < N} |Y_k|^2}{E\{|Y_n|^2\}}, \quad (3)$$

where  $E\{|Y_n|^2\}$  is the average power of the OFDM signal.

### B. Tone Injection

Tone injection suppresses the peak power by relocating some complex symbols from their original position to other position [6], [7]. Assume that the used digital modulation scheme is  $M$ -QAM with an  $\sqrt{M} \times \sqrt{M}$  constellation grid, and the minimum distance between constellation points is  $d$ . The original position of a complex symbol, which will be referred as original symbol, is located at a grid point of the  $\sqrt{M} \times \sqrt{M}$  grid, and the destination of relocation is located outside of the grid. In Fig.2, the original symbols for 16-QAM are shown as 16 black circles. Let the original position of a complex symbol representing a bit sequence  $\mathbf{b}_n = (b_{L-1}, b_{L-2}, \dots, b_0)$  be  $X_n$ . In [6], the set of complex symbols  $\hat{X}_n$  representing  $\mathbf{b}_n$  is given by the following equation:

$$\hat{X}_n = X_n + p_n D + j q_n D, \quad (4)$$

where  $D = \rho d M$ ,  $\rho \geq 1$  and  $p_n$  and  $q_n$  are any integer numbers. For  $p_n = q_n = 0$ ,  $\hat{X}_n$  is the original symbol  $X_n$ . For  $p_n \neq 0$  and/or  $q_n \neq 0$ ,  $\hat{X}_n$  is a relocated symbol,

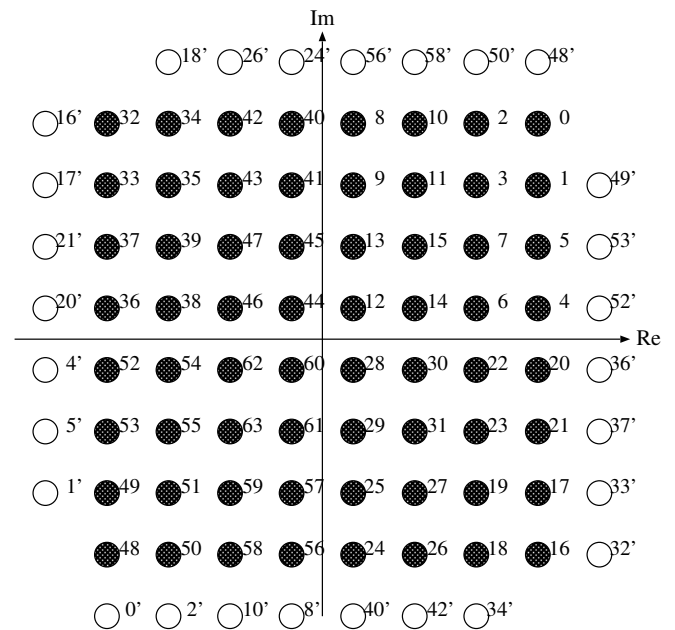


Fig. 3. The Used Constellation Map of 64-QAM

which is located outside of the  $\sqrt{M} \times \sqrt{M}$  grid. In Fig.2, the relocated symbols from  $X_n = -\frac{d}{2} + j\frac{3d}{2}$  for  $\rho = 1$ ,  $|p_n| \leq 1$  and  $|q_n| \leq 1$  are shown as 9 white circles.

The PAPR reduction task based on tone injection is to determine  $p_n$  and  $q_n$ , for all  $n$ , so as to minimize PAPR. That is, the task is a combinatorial optimization problem. However, the number of solutions are enormous even if the range of  $p_n$  and  $q_n$  are limited. Therefore, A greedy algorithm proposed in [6] is as follows:

(Step 1) Find the complex symbol  $X_n$  or  $\hat{X}_n$  that most contributes to the peak power.

(Step 2) Find the most effective  $p_n$  and  $q_n$  for PAPR reduction by evaluating all the combinations. Move the symbol  $X_n$  or  $\hat{X}_n$  according to the found  $p_n$  and  $q_n$ .

(Step 3) Repeat steps 1 and 2 until obtaining a sufficient PAPR reduction.

The following drawbacks of this method have been noted [6], [7]: (1) any average power increases results in a reduction in SNR margin, (2) unnecessary power increases can lead to higher secondary peaks, and (3) the greedy searching algorithm tends to get a stack shallow local minimum, which will result in a poor PAPR reduction performance.

In [7], two constraints, which are effective to relax the above drawbacks (1) and (2), have been introduced in peak power reduction based on tone injection. The constraints are as follows: (a) movable symbols are limited to the symbols located along the outer circumference of the original constellation, and (b) for a movable symbol the destination of relocation is limited to one place, which is an almost symmetrical position of the original position with respect to the origin. The constraints (a) and (b) will reduce the peak powers of subcarriers compared with the one without the constraints, because the magnitude of any complex symbol with the constraints is not larger than the one without the constraints. Further, the constraint (a) is validated by the observation that the outer circumferential symbols will contribute more to the peak power than the inner symbols.

In this paper, we also introduce the above constraints and use the constellation map of 64-QAM as shown in Fig.3. In Fig.3, the original symbols are shown as 64 black circles and the relocated symbols are shown as 28 white circles. In the figure, the black circle with a number  $m \in \{0, 1, \dots, 63\}$  is the original symbol  $X^{(m)}$ , and the white circle with a number  $m'$  is the replacement of the original symbol  $X^{(m)}$ .

Although the above constraints reduce the solution spaces, the number of solutions is still enormous. Assuming that  $N$  symbols to be transmitted randomly occur, the average number of solutions is  $2^{\frac{7}{16}N}$ , which is approximately  $5.2 \times 10^{33}$  and  $2.7 \times 10^{67}$  for  $N = 256$  and  $512$ , respectively. As a solution against the drawback (3), we will present a searching algorithm based on GA in the next section.

### III. PROPOSED METHOD

We apply genetic algorithm (GA) to the peak power reduction method based on tone injection. The GA, which is a search heuristic based on the process of natural evolution, can find a good solution for optimization problems by evolving the population of solutions with genetic operators such as selection, mutation and crossover[8]. GAs have been employed for solving many combinatorial optimization problems in various fields[9], [10], [11], [12], and it has been shown that GAs can find a near-optimal solution in a much shorter time compared to the conventional methods such as random search and exhaustive one, especially in large solution spaces. The proposed method uses GA to find an effective combination of symbols to be moved for PAPR reduction.

#### A. Genetic Representation

In GA, a solution is coded as a string, called chromosome. Let  $\mathcal{A} = \{X^{(0)}, X^{(1)}, \dots, X^{(M-1)}\}$  be the set of all the original complex symbols. Let  $\mathcal{M}$  be the set of the movable original complex symbols. That is, for Fig.3,  $\mathcal{M} = \{X^{(0)}, X^{(1)}, X^{(2)}, X^{(4)}, X^{(5)}, X^{(8)}, X^{(10)}, X^{(16)}, X^{(17)}, X^{(18)}, X^{(20)}, X^{(21)}, X^{(24)}, X^{(26)}, X^{(32)}, X^{(33)}, X^{(34)}, X^{(36)}, X^{(37)}, X^{(40)}, X^{(42)}, X^{(48)}, X^{(49)}, X^{(50)}, X^{(52)}, X^{(53)}, X^{(56)}, X^{(58)}\}$ .

Let  $\mathbf{X} = (X_0, X_1, \dots, X_{N-1})$  be the vector of original complex symbols to be transmitted. Let  $\mathcal{S} = \{X_n \in \mathcal{M} | 0 \leq n \leq N-1\}$  and  $S = |\mathcal{S}|$  be the set of movable symbols in  $\mathbf{X}$  and the size of  $\mathcal{S}$ , respectively. Let  $n(s)$  be the function of integer  $s \in \{1, 2, \dots, S\}$  such that  $|\{X_i \in \mathcal{M} | 0 \leq i \leq n(s)\}| = s$  and  $X_{n(s)} \in \mathcal{M}$ . That is, the function  $n(s)$  returns the  $s$ -th smallest index number  $n$  of  $X_n$  among  $\{X_n \in \mathcal{M} | 0 \leq n \leq N-1\}$ .

A solution (chromosome) for  $\mathbf{X}$  is coded as an  $S$ -dimensional binary vector

$$\mathbf{l} = (l_1, l_2, \dots, l_S), \quad (5)$$

where  $l_s \in \{0, 1\}$ , and  $l_s = 1$  and  $l_s = 0$  mean that the symbol  $X_{n(s)}$  is moved and is not moved, respectively. Fig.4 shows an example of the chromosome coding. Note that the length of a chromosome depends on  $\mathbf{X}$ . When the symbols to be transmitted randomly occur, the average length is  $\frac{7}{16}N$ .

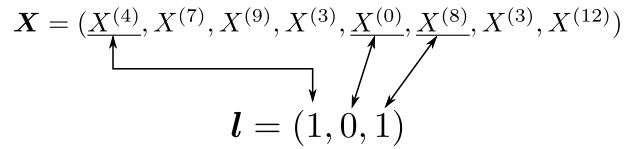


Fig. 4. An Example of Chromosome for  $N = 8$  and  $S = 3$

#### B. Fitness Function

When PAPR by Eq.(3) is used as evaluation function, a smaller PAPR value means a better solution. In order that a better solution has a larger evaluation value, we use the following evaluation function as GA's fitness function:

$$f = \left( \frac{1}{\text{PAPR}} \right)^\alpha, \quad (6)$$

where PAPR is calculated by Eq.(3) and  $\alpha > 0$  is a constant value that controls the degree of convergence. A larger  $\alpha$  makes the convergence faster. An effective value for  $\alpha$  is given by simulation in the next section.

#### C. Mutation and Crossover Operators

The used mutation operator operates on each locus of chromosomes. Given a chromosome  $\mathbf{l} = (l_1, l_2, \dots, l_S)$ , each locus  $l \in \{l_1, l_2, \dots, l_S\}$  is updated as follows:

$$l \leftarrow \begin{cases} (l+1) \bmod 2 & \text{with probability } P_m \\ l & \text{with probability } 1 - P_m. \end{cases} \quad (7)$$

Another approach is to perform the mutation for each chromosome. However, according to our preliminary simulation, this approach is not good.

We consider four types of crossover operator: one-point, two-point, three-point and uniform. For every types, the crossover points are randomly selected.

#### D. Fitness Table

The evaluation of a solution involves IFFT operation, which requires  $O(N \log N)$  steps. In order to reduce the computation time, the proposed algorithm utilizes a fitness table. Once a solution is evaluated, its fitness value is registered in the table. When thereafter the same solution appears, its fitness value is obtained by referring to the table instead of by calculation. We present two types of implementation of the fitness table: tree-structured[13] and hash-based ones.

1) *Tree-Structured Table*: If the search time is much smaller than the one of IFFT, a significant reduction of the computation time will be achieved. The fitness table also should be efficient in terms of memory. Therefore, in the first type of implementation of the fitness table, we use a binary tree[13]. The binary tree is as follows: (1) the height is  $S$ , (2) an edge between levels  $s-1$  and  $s$  ( $1 \leq s \leq S$ ) is associated with  $l_s$ , (3) for each node at level  $s-1$ , the left and right edges are associated with  $l_s = 0$  and  $l_s = 1$ , respectively, (4) the existence of the path corresponding to a solution  $\mathbf{l} = (l_1, l_2, \dots, l_S)$  means that the fitness value of  $\mathbf{l}$  is already registered, and (5) the fitness value of a solution  $\mathbf{l}$  is memorized in the leaf node of the path corresponding to  $\mathbf{l}$ . An example of the tree-structured table is shown in Fig.5. Since the search and the registration of the fitness value of

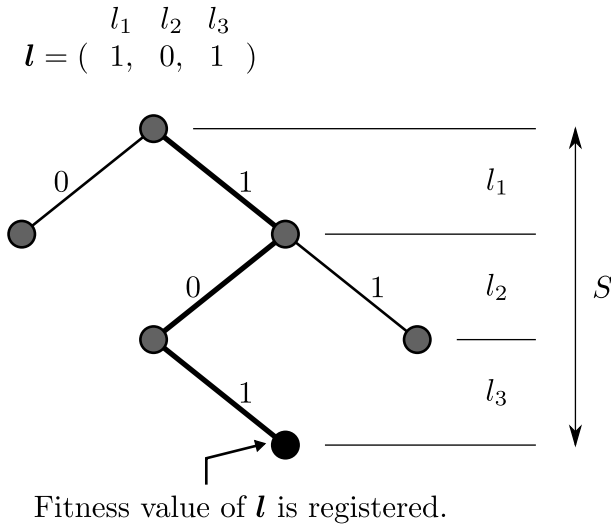


Fig. 5. An Example of the Tree-Structured Fitness Table for  $S = 3$  (the Bold Lines Show the Path of the Solution  $l$ )

a solution  $l$  trace from the root node to the corresponding leaf node, they completes in at most  $S$  steps. As mentioned before, the average of  $S$  is  $\frac{7}{16}N$ . Therefore, the search and the registration of a fitness value completes in  $O(N)$  steps.

2) *Hash-Based Table*: The second implementation of the fitness table uses a hash table. The hash table would be more effective than the tree-structured one in terms of search and insertion time. Because searching or inserting an item in a hash table can be done in  $O(1)$  steps if the table is well designed.

Fig.6 shows an example of the proposed hash-based fitness table for  $S = 3$  and  $B = 4$ , where  $B$  is the number of buckets. In the hash table, a solution  $l = (l_1, l_2, \dots, l_S)$  is mapped to  $h(l_1, l_2, \dots, l_{\log_2 B})$ -th bucket, where  $h(l_1, \dots, l_{\log_2 B})$  is the hash function as follows:

$$h(l_1, \dots, l_{\log_2 B}) = \sum_{i=1}^{\log_2 B} 2^{i-1} l_i. \quad (8)$$

The fitness value of  $l$  is stored with  $(S - \log_2 B)$ -bit number  $(l_{\log_2 B+1}, \dots, l_S)$  in the list of  $h(l_1, \dots, l_{\log_2 B})$ -th bucket. Note that if  $r$  different solutions stored in the hash table take a same hash value  $h(l_1, \dots, l_{\log_2 B})$ , the length of the list corresponding to  $h(l_1, \dots, l_{\log_2 B})$ -th bucket is  $r$ .

The access time to the target bucket is always  $O(1)$ , because the bucket is an element in an array and the address of the target bucket is given by the subsequence of the bits in  $l$ . The search and insertion time on the list is proportional to the length of the list. However, if the number of buckets  $B$  is sufficiently large, i.e.  $O(S)$ , the total search and insertion time is  $O(1)$ .

### E. The Algorithm

The algorithm of the proposed GA is shown below. The fitness table used in Step 3 is implemented by a tree-structured or hash-based table described in subsection III-D.

#### Algorithm

**Step 1:** Set the current generation  $g \leftarrow 1$ . Set the best fitness  $f_{\text{best}} \leftarrow 0$ .

$$\begin{aligned} l_a &= \begin{pmatrix} l_1 & l_2 & l_3 \\ 0 & 0 & 1 \end{pmatrix} \\ l_b &= \begin{pmatrix} 1 & 0 & 0 \end{pmatrix} \\ l_c &= \begin{pmatrix} 1 & 0 & 1 \end{pmatrix} \end{aligned}$$

$S = 3$

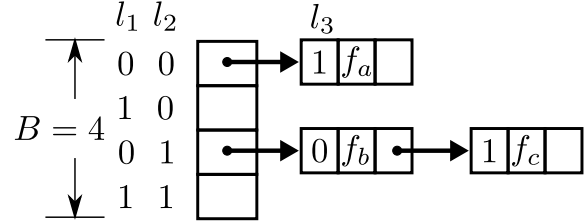


Fig. 6. An Example of the Hash-Based Fitness Table for  $S = 3$  and  $B = 4$  ( $f_a$ ,  $f_b$  and  $f_c$  are the Fitness Values for  $l_a$ ,  $l_b$  and  $l_c$ , Respectively)

**Step 2:** Randomly generate  $K$  individuals  $l_1, l_2, \dots, l_K$  in the form of Eq.(5).

**Step 3:** For each  $k \in \{1, 2, \dots, K\}$ , search for the fitness  $f_k$  in the fitness table. If  $f_k$  is not found, calculate  $f_k$  according to Eq.(6), and register  $f_k$  into the fitness table.

Let  $f_{\text{max}} = \max_{k \in \{1, 2, \dots, K\}} f_k$ . Let  $k_{\text{max}} \in \{1, 2, \dots, K\}$  such that  $f_{k_{\text{max}}} = f_{\text{max}}$ . If  $f_{\text{max}} > f_{\text{best}}$ , then  $f_{\text{best}} \leftarrow f_{\text{max}}$  and  $l_{\text{best}} \leftarrow l_{k_{\text{max}}}$ .

**Step 4:** If  $g > G$ , then go to Step 10.

**Step 5:** For each  $k \in \{1, 2, \dots, K\}$ , calculate the selection probability

$$P_k = \frac{f_k}{\sum_{i \in \{1, 2, \dots, K\}} f_i}.$$

Draw  $K$  samples  $l'_1, l'_2, \dots, l'_K$  with replacement from  $l_1, l_2, \dots, l_K$  with probabilities  $P_1, P_2, \dots, P_K$ .

**Step 6:** For each pair  $l'_{2k+1}$  and  $l'_{2k+2}$  ( $0 \leq k \leq \frac{K}{2} - 1$ ), perform the crossover operation with probability  $P_c$ .

**Step 7:** For each locus  $l_s$  in  $l'_1, l'_2, \dots, l'_K$ , perform the mutation operation with probability  $P_m$ .

**Step 8:** Copy  $l'_1, l'_2, \dots, l'_K$  to  $l_1, l_2, \dots, l_K$ , respectively.

**Step 9:**  $g \leftarrow g + 1$  and go to Step 3.

**Step 10:** Return  $l_{\text{best}}$  as the final solution.  $\square$

In GA, as the generation progresses, the large portion of the population converges to particular solutions. This property will make it possible for Step 3 to reduce the computation time.

In Step 6, one of the four types of crossover operator is used. The best type will be shown in the next section.

## IV. NUMERICAL SIMULATIONS

The simulations assume an AWGN (Additive White Gaussian Noise) channel, where a white noise with SNR 20dB is added to the signal from the amplifier. The used nonlinear power amplifier model has the following input-output characteristic.

$$F[\rho] = \frac{\rho}{(1 + \rho^6)^{1/6}}, \quad (9)$$

where  $F[\rho]$  is the gain of the amplifier and  $\rho$  is the ratio of the mean input amplitude to the saturation amplitude.

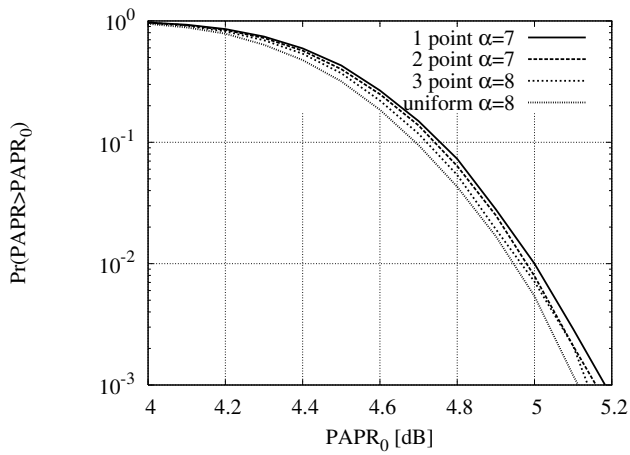


Fig. 7. PAPR for Different Crossover Methods

The number of subcarriers is  $N = 128$ , the population size is  $K = 30$ , the maximum generation number is  $G = 50$ , and the probabilities for crossover and mutation are  $P_c = 0.9$  and  $P_m = 0.01$ , respectively. Each result is calculated from 100000 trials.

#### A. PAPR Reduction Performance

At first, for each crossover operator type, the effective value of parameter  $\alpha$  in the fitness function is investigated in terms of PAPR. From the results, for 1-point, 2-point, 3-point and uniform crossovers, the best values for  $\alpha$  are  $\alpha = 7$ ,  $\alpha = 7$ ,  $\alpha = 8$  and  $\alpha = 8$ , respectively.

The results with the best  $\alpha$  are summarized in Fig.7.  $PAPR_0$  at the horizontal axis is the upper limit of the linear amplification range, and  $\Pr(PAPR > PAPR_0)$  at the vertical axis is the probability that PAPR exceeds the limit  $PAPR_0$ . This figure shows a tendency that the PAPR reduction performance improves with the number of crossover points and the uniform crossover operator provides the best performance. Therefore, in the following, the proposed method assumes to use uniform crossover and  $\alpha = 8$ .

Next, the proposed method is compared with a conventional method based on neural network (NN)[7] and a random search. The result is shown in Fig.8. In the figure, “NN”, “Random” and “Proposed” are the method based on NN (NN method), a random search and the proposed method, respectively. All the methods use the same constellation map shown in Fig.3. The random search randomly generates 1500 solutions and returns the best solution as the final solution. According to the result, the proposed method achieves the best performance among them.

#### B. Bit Error Rate Performance

The proposed GA method is compared with the conventional NN method and the random search in terms of bit error rate (BER).

$$BER = \frac{(\text{Total number of error bits})}{(\text{Total number of transmitted bits})} \quad (10)$$

The result is shown in Fig.9, where IBO (Input Back-Off) defines the degree of nonlinearity of an amplifier and is given

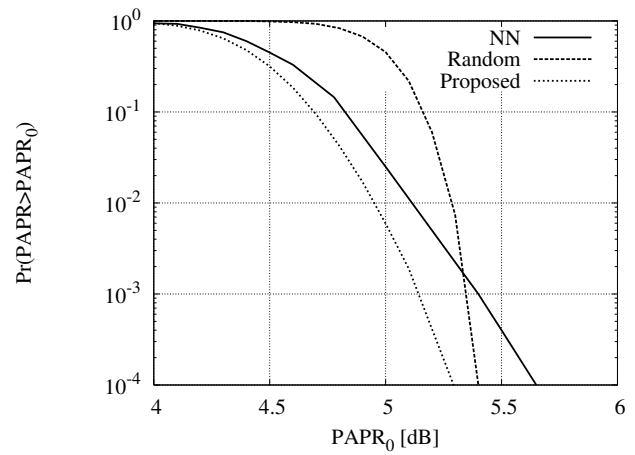


Fig. 8. Performance Comparison of PAPR Reduction with Conventional Methods

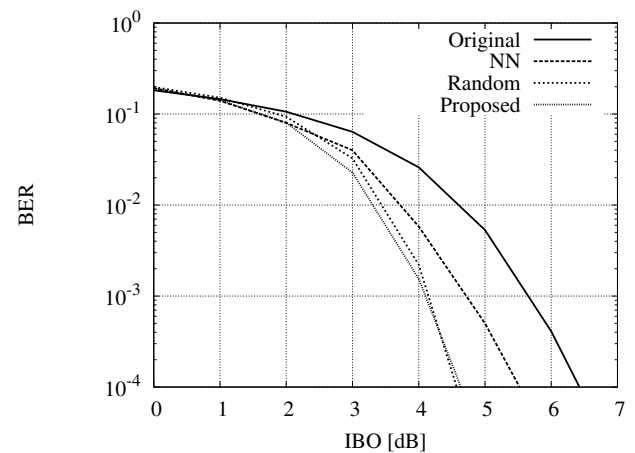


Fig. 9. BER Performance

by the following equation.

$$IBO = \frac{(\text{Saturation amplitude})}{(\text{Mean input power})} \quad (11)$$

In Fig.9, “Original” is the case of no PAPR reduction. The result shows that the proposed method achieves the best BER performance.

#### C. Power Spectrum Density

The proposed GA method is compared with the conventional NN method and the random search in terms of power spectral density (PSD) of OFDM signal passing through a nonlinear amplifier. The result is shown in Fig.10. In the figure, “amp+” indicates that the OFDM signal is passed through a nonlinear amplifier with IOB 5.0dB, and “linear amp” indicates that the OFDM signal is passed through a linear amplifier and tone injection is not applied. The PSD should be minimized when the normalized frequency is more than 1.0. Therefore, the proposed GA is most effective among all the methods.

#### D. Computation Time

We measure the computation time for random search, conventional GA and two types of the proposed GA. The

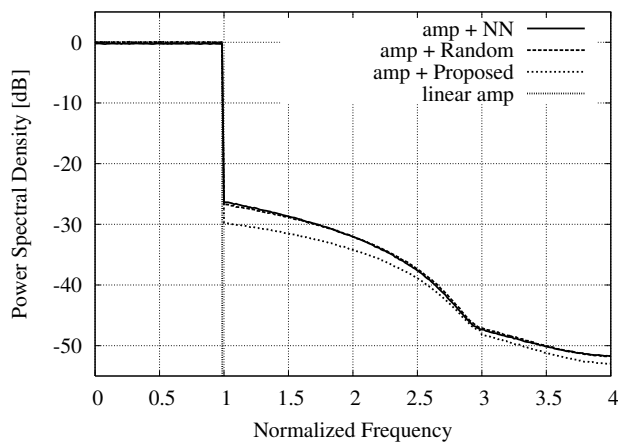


Fig. 10. Power Spectral Density (PSD)

TABLE I  
THE COMPUTATION TIME IN CPU TIME (MSEC)

Random search	GA		
	Without table	Tree	Hash
35.2	36.2	23.0	21.4

conventional GA does not use the fitness table and calculates the fitness for all the individuals. The proposed GA method uses a tree-structured or hash-based fitness table. The computation time is calculated in terms of CPU time. The result is shown in table I. According to the result, the hash-based fitness table is more effective than the tree-structured one. The result also show that our proposed method achieve about 1/3 reduction in the computation time. The total number of unique individuals occurring through all the generations of GA is approximately 1000. Since the total number of individuals through all the generations is 1500, the amount of reduction in the computation time is proportional to the amount of the duplicated individuals.

## V. CONCLUSIONS

In this paper, we applied GA to the peak power reduction method based on tone injection. The proposed GA method utilized a fitness table to reduce the computation time. For the fitness table, two types of implementation were presented. We tested four types of crossover operators: one-point, two-point, three-point and uniform crossovers. The result showed that the PAPR reduction performance improves with the number of crossover points and the uniform crossover operator provides the best performance. The GA method was compared with the conventional NN method and a random search in terms of PAPR, BER and PSD. The result showed that the GA method is superior compared to the conventional NN method and the random search. Further, our GA method using fitness table was compared with random search and conventional GA in terms of the computation time. The result showed that our GA method is faster than conventional GA and that the hash-based fitness table is more effective than the tree-structured one.

## REFERENCES

- [1] Weinstein, S., Ebert, P., "Data Transmission by Frequency-Division Multiplexing Using the Discrete Fourier Transform," *IEEE Trans. on Communication Technology*, Vol.19, Issue 5, pp.628-634, 1971.
- [2] Li, X., Cimini, L.J., Jr., "Effects of Clipping and Filtering on the Performance of OFDM," *IEEE Communications Letters*, Vol.2, No.5, pp. 131-133, 1998.
- [3] Armstrong, J., "New OFDM Peak-to-Average Power Reduction Scheme," *Proc. of IEEE Vehicular Technology Conference*, pp. 756-760, 2001.
- [4] Jones, A.E., Wilkinson, T.A., Barton, S.K., "Block Coding Scheme for Reduction of Peak to Mean Envelope Power Ratio of Multicarrier Transmission Scheme," *Electronics Letters*, Vol.30, No.25, pp.2098-2099, 1994.
- [5] Cimini, L.J., Jr., Solenberger, N.R., "Peak-to-Average Power Ratio Reduction of an OFDM Signal Partial Transmit Sequences," *IEEE Communications Letters*, Vol.4, No.3, pp. 86-88, 2000.
- [6] Tellado, J., Cioffi, J., "Peak Power Reduction for Multicarrier Transmission," *Proc. of IEEE Communication Theory Mini-Conference, GLOBECOM '98*, pp.219-224, 1998.
- [7] Ohta, M., Ueda, Y., Yamashita, K., "PAPR Reduction of OFDM Signal by Neural Networks without Side Information and its FPGA Implementation," *IEEJ Trans. on Electronics, Information and Systems* (in Japanese), Vol.126, No.11, pp. 1296-1303, 2006.
- [8] Goldberg, D.E., *Genetic Algorithms in Search, Optimization and Machine Learning*, Kluwer Academic Publishers, 2002.
- [9] Kitabi, A., Jenkins, W.K., "Use of the Genetic Algorithm to Improve Bit Error Rates in CDMA Wireless Communication Systems," *Conference Record of the Thirty-Fifth Asilomar Conference on Signals, Systems and Computers*, Vol.2, pp.1540-1544, 2001.
- [10] Thamvichai, R., Bose, T., Haupt, R.L., "Design of 2-D Multiplierless IIR Filters Using the Genetic Algorithm," *IEEE Trans. on Circuit and Systems-I: Fundamental and Applications*, Vol.49, No.6, pp.878-882, 2002.
- [11] Li, Y., Ang, K.H., Chong, G.C.Y., Feng, W., Tan, K.C., Kashiwagi, H., "CAutoCSD-Evolutionary Search and Optimisation Enabled Computer Automated Control System Design," *International Journal of Automation and Computing*, Vol.1, No.1, pp.76-88, 2004.
- [12] Gondro, C., Kinghorn, B.P., "A Simple Genetic Algorithm for Multiple Sequence Alignment," *Genetics and Molecular Research*, Vol.6, No.4, pp. 964-982, 2007.
- [13] Shigei, N., Miyajima, H., Ozono, K., "Time-Efficient Genetic Algorithm for Peak Power Reduction of OFDM Signal," *Lecture Notes in Engineering and Computer Science: Proceedings of The World Congress on Engineering and Computer Science 2010, WCECS 2010*, 20-22 October, 2010, San Francisco, USA, pp. 186-191.